The Distributional Effects of Economic Uncertainty

Florian Huber
University of Salzburg
Massimiliano Marcellino
Bocconi University, CEPR, IGIER
Tommaso Tornese
Bocconi Univeristy

NBER Summer Institute, 11 July 2024

Motivation

- Uncertainty among drivers of the business cycle (e.g. Castelnuovo, 2019; Fernández-Villaverde and Guerrón-Quintana, 2020);
- Extensive literature on the aggregate effects of uncertainty shocks (e.g. Bloom, 2009; Jurado et al., 2015; Carriero et al., 2021; Carriero et al., 2023);

- **Limited research on the distributional implications;**

- Growing attention towards distributional aspects of macroeconomic phenomena:
  - Aggregate effects of distributional dynamics (e.g. Heathcote et al., 2010; Athreya et al., 2017; and Auclert et al., 2020);
  - Distributional implications of aggregate shocks (e.g. Anderson et al., 2016; De Giorgi and Gambetti, 2017; Ahn et al., 2018; Kaplan and Violante, 2018).

Motivation

- Modeling distributional dynamics using standard methods is problematic:
  - Percentiles in standard VARs $\Longmapsto$ percentiles crossing;
  - Moments in standard VARs $\Longmapsto$ number of moments is indefinite;
- A distribution is a function (infinite-dimensional vector):
- Growing interest towards statistical methods for functional data (observations of curves defined on a continuous domain). Examples:
  - Electricity consumption (e.g. Ferraty and Vieu 2006);
  - Yield curve (e.g. Litterman and Scheinkman 1991; Diebold and Li, 2006);
  - Distribution of high frequency stock prices (Tsay, 2016).

Related literature

- Use of Functional-VAR to model joint dynamics of aggregate variables and income distribution (e.g. Chang M. et al., 2024).
- Econometric methods for functional data:
  - Bayesian (Kowal et al., 2017; Chang M. et al., 2024);
  - Frequentist (Chang et al., 2016; Hu and Park, 2016);
- Recent empirical applications of functional models:
  - Inoue and Rossi (2018): monetary policy as functional schocks;
  - Meeks and Monti (2023): Phillips curve with heterogeneous beliefs;
  - Chang et al. (2022): effects of shocks on heterogeneous inflation expectations;
  - Bjørnland et al.(2023): effects of oil shocks on the distribution of stock returns;
  - Chang and Schorfheide (2024): effects of monetary policy on earnings/consumption distribution.

Contribution

- How to treat distributions for Functional Data Analysis (FDA): different transformations have different pro and cons;
- How to summarize the density through Functional-PCA (FPCA, Ramsay and Silverman, 1997): advantages over alternative methods (e.g. splines, Chang et al., 2024);
- What are the effects of uncertainty shocks on income distribution;
- Robustness of the results to different modeling strategies;
- Estimation of the effects through Functional Local Projections.

Preview of the results

- Show through simulations that:
    - FPCA on $p_t(\cdot)$ provides best approximations, but produces inadmissible distribution responses to shocks (i.e. densities with negative regions);
    - FPCA on $\log(p_t(\cdot))$ ensures non-negativity (not unit-integration) of distributions, but provides worst approximations;
    - FPCA on Log Quantile Density (LQD, Petersen and Muller, 2016) ensures non-negativity and unit-integration of distributions, and provides accurate approximations;
- Propagation of uncertainty shocks in two phases (Carriero et al, 2024):
    - Short run: Unemployment increases, in particular for less educated workers; Investments are reduced; Share of employed with low relative income decreases $\Longmapsto$ Decreased inequality among employees;
    - Longer horizon: Unemployment is reabsorbed, especially among less educated workers; Labor productivity decreases; Mass of low-income workers increases $\Longmapsto$ Increased inequality among employees.

Outline of the presentation

1. Econometric Model:
    1. Functional VAR
    2. Density Estimation
    3. Transformation of the Density
    4. FPCA
    5. VAR Inference
2. Simulated Data Experiments
3. Effects of Uncertainty Shocks on Earnings Distribution
4. Functional Local Projections
5. Conclusions

The model

- Assume that income observations are $\xi_{it} \sim iid\ p_t$, $\xi_{it} \in \Xi$;
- Objective is to model the joint dynamics of:
  - A function, $p_t(\xi)$, defined on a continuous support Ξ;
  - A set of n_v random variables, $y_t = [y_{1,t}, ..., y_{n_v,t}]'$.
- Define $f_t(\xi) = g(p_t(\xi)) - \bar{g}$ to be some de-meaned transformation of the distribution (i.e. $\bar{g} = \frac{1}{T}\sum_{t=1}^{T} g(p_t(\xi)))$;
- Specify y_t to be a vector of macro/financial aggregate variables.

Functional VAR (F-VAR)

- The F-VAR(p) is (see e.g. Inoue and Rossi, 2021; Chang et al., 2024):

$$y_t = c_y + \sum_{l=1}^{p} B_{l,yy} y_{t-l} + \sum_{l=1}^{p} \int B_{l,yf}\left(\acute{\xi}\right) f_{t-l}\left(\acute{\xi}\right) d\acute{\xi} + u_{y,t}$$

$$f_t\left(\xi\right) = c_f\left(\xi\right) + \sum_{l=1}^{p} B_{l,fy}\left(\xi\right) y_{t-l} + \sum_{l=1}^{p} \int B_{l,ff}\left(\xi, \acute{\xi}\right) f_{t-l}\left(\acute{\xi}\right) d\widetilde{\xi} + u_{f,t}\left(\xi\right)$$

- Where $u_{y,t}$ and $u_{f,t}\left(\xi\right)$ are innovations with zero mean and variance:

$$\Omega(\xi, \acute{\xi}) = \begin{bmatrix} \Omega_{yy} & \Omega_{yf}\left(\acute{\xi}\right) \\ \Omega_{fy}\left(\xi\right) & \Omega_{ff}\left(\xi, \acute{\xi}\right) \end{bmatrix}.$$

Functional VAR (F-VAR)

- $f_t(\cdot)$ and $u_{f,t}(\cdot)$ are continuous functions $\Longmapsto$ Infinite dimensional model;
- By the Karhunen-Loéve theorem, every random function can be represented as an expansion in some orthogonal functional basis (e.g. splines, Fourier series, wavelets).
- The functions, $f_t(\cdot)$ and $u_{f,t}(\cdot)$ can then be written as:

$$f_t(\xi) = \sum_{k=1}^{\infty} \zeta_k(\xi) * \alpha_{k,t};$$

$$u_{f,t}(\xi) = \sum_{k=1}^{\infty} \zeta_k(\xi) * \widetilde{u}_{k,t};$$

where $\zeta_k(\cdot)$ are components of the functional basis, and $\alpha_{k,t}$ and $\widetilde{u}_{k,t}$ are scalars;

- We assume that these functions can be approximated by terminating the expansions at some truncation point, K:

$$f_t(\xi) \approx \sum_{k=1}^{K} \zeta_k(\xi) * \alpha_{k,t} = \boldsymbol{\zeta}'(\xi)\, \boldsymbol{\alpha}_t; \;\; u_{f,t}(\xi) \approx \sum_{k=1}^{K} \zeta_k(\xi) * \widetilde{u}_{k,t} = \boldsymbol{\zeta}'(\xi)\, \widetilde{\boldsymbol{u}}_t;$$

where $\zeta(\xi)$ is a $K \times 1$ vector of coefficients, and $\boldsymbol{\alpha}_t$ and $\widetilde{\boldsymbol{u}}_t$ are $K \times 1$ random vectors.

Functional VAR (F-VAR)

- Similarly, the functional coefficients, $c_f(\cdot)$, $B_{l,fy}(\cdot)$, $B_{l,yf}(\cdot)$, and $B_{l,ff}(\cdot,\cdot)$, can then be written as:

$$c_f(\xi) = \sum_{k=1}^{\infty} \zeta_k(\xi) * \widetilde{c}_{f,k}; \quad B_{l,fy}(\xi) = \sum_{k=1}^{\infty} \zeta_k(\xi) * \widetilde{\boldsymbol{b}}'_{l,fy,k};$$

$$B_{l,yf}\left(\acute{\xi}\right) = \sum_{j=1}^{\infty} \delta_j\left(\acute{\xi}\right) * \widetilde{\boldsymbol{b}}_{l,yf,j}; \; B_{l,ff}\left(\xi,\acute{\xi}\right) = \sum_{k=1}^{\infty}\sum_{j=1}^{\infty} \zeta_k(\xi) * \delta_j\left(\acute{\xi}\right) * \widetilde{b}_{l,ff,kj};$$

where $\delta_j(\cdot)$ are components of another functional basis,$\widetilde{c}_{f,k}$, and $\widetilde{b}_{l,ff,kj}$ are scalars, and $\widetilde{\boldsymbol{b}}_{l,fy,k}$ and $\widetilde{\boldsymbol{b}}_{l,yf,j}$ are $n_v \times 1$ vectors.

- Hence, we consider the approximations:

$$c_f(\xi) \approx \boldsymbol{\zeta}'(\xi)\,\widetilde{\boldsymbol{c}}_f; \quad B_{l,fy}(\xi) \approx \boldsymbol{\zeta}'(\xi)\,\widetilde{\boldsymbol{B}}_{l,fy};$$

$$B_{l,yf}\left(\acute{\xi}\right) \approx \widetilde{\boldsymbol{B}}'_{l,fy}\boldsymbol{\delta}(\xi); \; B_{l,ff}\left(\xi,\acute{\xi}\right) \approx \boldsymbol{\zeta}'(\xi)\,\widetilde{\boldsymbol{B}}_{l,ff}\boldsymbol{\delta}\left(\acute{\xi}\right);$$

where $\delta\left(\acute{\xi}\right)$ is a $K \times 1$ vector of coefficients, $\widetilde{\boldsymbol{c}}_f$, $\widetilde{\boldsymbol{B}}_{l.fy}$, $\widetilde{\boldsymbol{B}}_{l,fy}$ and $\widetilde{\boldsymbol{B}}_{l,ff}$ are matrices of parameters, of dimension $K \times 1$, $K \times n_v$, $n_v \times K$, and $K \times K$ respectively.

Functional VAR (F-VAR)

- Using this finite approximation, the F-VAR becomes a standard finite-dimensional Factor Augmented VAR:

$$\begin{bmatrix} y_t \\ \alpha_t \end{bmatrix} = \begin{bmatrix} c_y \\ \widetilde{\boldsymbol{c}}_f \end{bmatrix} + \sum_{l=1}^{p} \begin{bmatrix} B_{l,yy} & B_{l,yf}\, C_\alpha \\ B_{l,fy} & B_{l,ff}\, C_\alpha \end{bmatrix} \begin{bmatrix} y_{t-l} \\ \alpha_{t-l} \end{bmatrix} + \begin{bmatrix} u_{y,t} \\ \widetilde{u}_{f,t} \end{bmatrix},$$

where $C_\alpha \equiv < \boldsymbol{\delta}(\cdot), \boldsymbol{\zeta}(\cdot) > = \int \boldsymbol{\delta}\left(\acute{\xi}\right) \boldsymbol{\zeta}'\left(\acute{\xi}\right) d\acute{\xi}$, and $u_t = \left[u'_{y,t}, \widetilde{u}'_t\right]'$ has zero mean and variance Ω.

- Inference can now be performed applying conventional frequentist or Bayesian techniques;
- It can be given a structural interpretation based on identifying assumptions;
- Functional Impulse Response Functions (F-IRFs) can be computed by mapping back the IRFs for $\boldsymbol{\alpha}_t$ to the functional space using the basis $\zeta(\cdot)$.

Recursive Identification

- Assume that the VAR is driven by $n = n_v + K$ structural shocks, ε_t:

$$A_0 u_t = \varepsilon_t,$$

  with ε_t being i.i.d. with zero mean and diagonal variance Σ.

- If A_0 is assumed to be lower-triangular, the structural form of the F-VAR is (as usual) exactly identified;

- A_0 can be found by inverting the lower-triangular Cholesky factor of the estimated Ω;

- Note: the choice of $\zeta(\cdot)$ affects $\widetilde{u}_{f,t}$, but it does not affect the labeling of the first n_v structural shocks in ε_t, $\varepsilon_{y,t}$.

Functional IRFs

- Given the finite dimensional representation of the Functional-VAR, the IRFs of $\boldsymbol{\alpha}_{\mathrm{t}}$ at horizon h after a shock $\varepsilon_j = d$, $IRF_\alpha\left(h, \varepsilon_j = d\right)$, can be easily computed;
- These need to be mapped back to IRFs for the distribution of interest, $IRF_p\left(h, \varepsilon_j = d\right)$, by:
  1. Computing the model-implied steady-state distribution:
  $$p_{ss}\left(\cdot\right) = g^{-1}\left(\zeta\left(\cdot\right)' \boldsymbol{\alpha}_{ss} + \bar{g}\right)$$
  2. Computing the expected distribution h periods after the shock:
  $$p_{ss+h}\left(\cdot\right)|_{\varepsilon_j=d} = g^{-1}\left(\zeta\left(\cdot\right)' \left(\boldsymbol{\alpha}_{ss} + IRF_\alpha\left(h, \varepsilon_j = d\right)\right) + \bar{g}\right)$$
  3. Computing the difference between the two:
  $$IRF_p\left(h, \varepsilon_j = d\right) = p_{ss+h}\left(\cdot\right)|_{\varepsilon_j=d} - p_{ss}\left(\cdot\right)$$

FDA on Distributions

Performing FDA on distributions poses unique challenges:

- Ignore constraints: $f_t(\xi) = p_t(\xi) - \frac{1}{T}\sum_{t=1}^{T} p_t(\xi)$ (i.e. $g(p_t(\cdot)) = p_t(\cdot)$):
  - PRO: Enforces unit integration of $p_{ss+h}(\cdot)|_{\varepsilon_j=d}$ and $p_{ss}(\cdot)$ if $\zeta(\cdot)$ have zero integral. Allows good approximation in terms of Euclidean distance;
  - CONS: If $\zeta(\cdot)$ have zero integral, F-IRFs can leave the space of densities (i.e. can take negative values in some regions of the support);
- Consider $f_t(\xi) = \log(p_t(\xi)) - \frac{1}{T}\sum_{t=1}^{T} \log(p_t(\xi))$ (i.e. $g(p_t(\cdot)) = \log p_t(\cdot)$):
  - PRO: Enforce non negativity constraint;
  - CONS: $p_{ss+h}(\cdot)|_{\varepsilon_j=d}$ and $p_{ss}(\cdot)$ need to be re-normalized to have unit integral. Approximation can be poor;
- Consider the Log Quantile Density (LQD) associated with $p_t(\xi)$ (Petersen and Müller, 2016):
  - PRO: It is unrestricted and can be easily mapped back to the pdf of interest for a given support. It is less sensitive to horizontal variation and to outliers;
  - CONS: The approximation can be less accurate than the one allowed by the first approach (although not always, see Petersen and Müller, 2016).

Log Quantile Density

$$g\left(p_t(\cdot)\right) = \log\left\{ \frac{d}{dz} Q_t(z) \bigg|_{z=x} \right\} = -\log\left\{ p_t\left(Q_t(x)\right)\right\}$$

where $Q(z) = F^{-1}(z)$ is the quantile function (inverse cdf), and $x \in [0,1]$.

- It loses information about Ξ, but is totally unrestricted (i.e. it lies in the linear L^2 space).
- When Ξ is known, $p_t(\cdot)$ can be easily dervided back from the LQD, by:
  1. Computing $Q_t(x) = \theta \int_0^x \exp\left[f_t(z)\right] dz$, where $\theta = \sup_{\xi \in \Xi} \xi \times \left\{\int_0^1 \exp\left[f_t(z)\right] dz\right\}^{-1}$;
  2. Computing $p_t(\xi) = \frac{d}{d\xi} F_t(\xi) = \frac{d}{dz} Q_t^{-1}(\xi)$.

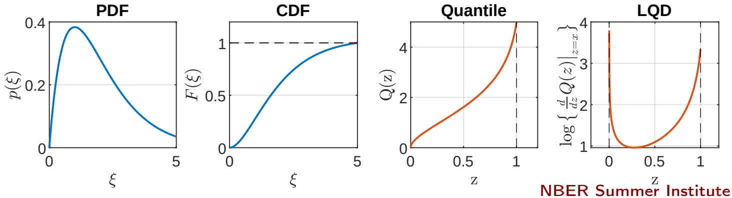

Functional Bases

- Choice of the bases $\zeta(\cdot)$ and $\delta(\cdot)$:
  - The choice of $\delta(\cdot)$ is irrelevant, as long as $C_\alpha = \int \boldsymbol{\delta}\left(\acute{\xi}\right)\boldsymbol{\zeta}'\left(\acute{\xi}\right)d\acute{\xi}$ is finite. It never appears in the analysis;
  - The choice of $\zeta(\cdot)$ is crucial:
    - Splines: Chang M. et al. (2022). Can need large K to summarize important features of $f_t(\cdot)$.
    - FPCA: Tsay (2016), Chen et al. (2019), Meeks and Monti (2021). The shape of the components $\zeta_k(\cdot)$ are automatically selected to reflect the most important features for the dynamics of $f_t(\cdot)$.

- We use Tsay's (2016) FPCA approach:
  - Summarizes the bulk of the dynamic variation observed in $f_t(\cdot)$ with low K;
  - Easy to implement;
  - We experimented with other methods with no meaningful changes.

Empirical Approach

- We follow a three-step approach:

1. Estimate the distribution of interest for every t from a sample of draws;
2. Transform the distributions and approximate the resulting function through FPCA;
3. Jointly model the FPCs and a set of random variables with a (Bayesian) VAR.

Density Estimation

- We estimate the distribution of interest (income) using a kernel density estimator (Venables and Ripley, 1999);

- We adopt a boundary correction as the support of the distribution is bounded;
- The kernel estimator is:

$$\hat{p}_t\left(\xi\right) = \frac{1}{n_t h}\sum_{i=1}^{n_t}\left\{\Phi\left(\frac{\xi-\xi_{it}}{h}\right)+\Phi\left(\frac{\xi-\xi_{it}^L}{h}\right)+\Phi\left(\frac{\xi-\xi_{it}^U}{h}\right)\right\};$$

  where $\xi_{it}^L = 2L - \xi_{it}$ and $\xi_{it}^U = 2U - \xi_{it}$, with L and U being the lower and upper bound of the support. Φ is the Gaussian kernel, h is the bandwidth, and n_t is the size of the sample drawn from p_t.
- We set h following Silverman's rule of thumb.

Functional Principal Component Analysis (FPCA)

- Let X denote a $T \times N$ matrix with $(t, i)^{th}$ element $x_{t,i} = f_t(\xi_i) = g(\hat{p}_t(\xi_i))$, $t = 1, ..., T$, $i = 1, ..., N$.
- The matrix X can be decomposed using a truncated Singular Value Decomposition (SVD, see e.g. Tsay, 2016):

$$X = SVD' + E;$$

  where:
  - S is the $T \times K$ matrix of the first K left eigenvectors;
  - V is the $K \times K$ diagonal matrix containing the largest K eigenvalues;
  - D is the $N \times K$ matrix of the first K right eigenvectors;
  - E contains the approximation error for considering only K components.
- The principal components D will serve as our functional basis $\zeta(\cdot)$;
- The scores VS_t' (S_t: t-th row of S), will serve as our factors $\boldsymbol{\alpha}_t$;
- The estimated $\hat{\boldsymbol{\alpha}}_t$ can be plugged in the $n_v + K$-dimensional VAR.
- FPCA selects the modes of variation that explain the largest share of time vatiation in $f_t(\xi_i)$ (i.e. they are more effcient than alternative bases).

Inference

- Standard Bayesian or frequentist methods can be applied to perform inference on the $n_v + K$-dimensional VAR:

$$z_t = \Pi x_t + u_t,$$

where $z_t = [y_t', \alpha_t']'$, $x_t = \left[1, z_{t-1}', \ldots, z_{t-p}'\right]'$ and $\Pi = [\Pi_0, \Pi_1, \ldots, \Pi_p]$, with $\Pi_0 = \left[c_y', \tilde{c}_f'\right]'$ and $\Pi_l = \begin{bmatrix} B_{l,yy} & B_{l,yf} C_\alpha \\ B_{l,fy} & B_{l,ff} C_\alpha \end{bmatrix}$.

- In all applications, we use Bayesian methods and assume natural conjugate Gaussian-Inverse Wishart prior distribution for the reduced form parameters (Π, Ω): $p\left(vec\left(\Pi'\right), \Omega\right) = p\left(\Omega\right) \times p\left(vec\left(\Pi'\right) \mid \Omega\right)$,
    - $p\left(\Omega\right)$ is Inverse Wishart with ν degrees of freedom and scale matrix Φ;
    - $p\left(vec\left(\Pi'\right) \mid \Omega\right)$ is Gaussian with mean $vec\left(\Psi\right)$ and variance $\Omega \otimes \Gamma$;
- We set ν, Φ, Ψ,and Γ following the Minnesota tradition (Doan et al., 1984; Carriero et al., 2015).

Simulated Data 1: F-SVAR DGP 1

1. Simulate $T = 500$ data points, z_t, from a $n_v + K_{true}$-dimensional SVAR(p), with: lower triangular A_0, $p = 4$, $n_v = 2$, and $K_{true} = 3$;
2. Simulated α_t are transformed into LQD functions, using as basis the FPC taken from the LQD of a mixture of *Gammas*, with a time varying *Beta* mixing distribution;
3. The LQDs are then transformed into distributions with support $\Xi = [0, 6]$;
4. A sample of size $N = 500$ is drawn at every t and assumed observed by the econometrician.

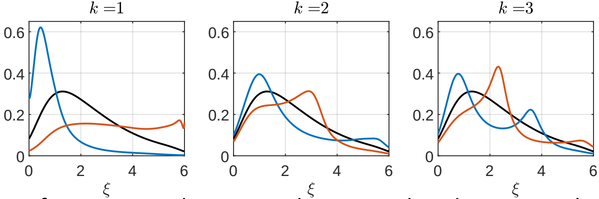

DGP's modes of variation: change to the mean distribution implied by a 2 std change in $\alpha_{k,t}$ (red: positive, blue: negative).

Simulated Data 2: F-SVAR DGP 2

1. Simulate $T = 500$ data points, z_t, from a $n_v + K_{true}$-dimensional SVAR(p), with: Lower triangular A_0, $p = 4$, $n_v = 2$, and$K_{true} = 3$;
2. Simulated α_t are transformed into $p_t(\cdot)$, using as basis the FPC taken from a mixture of *Gammas*, with a time varying *Beta* mixing distribution;
3. At every t, $N = 500$ draws are taken from $p_t(\cdot)$, which is obtained by taking the exponential of $\log(p_t(\cdot))$ and re-normalizing it to have unit integral.

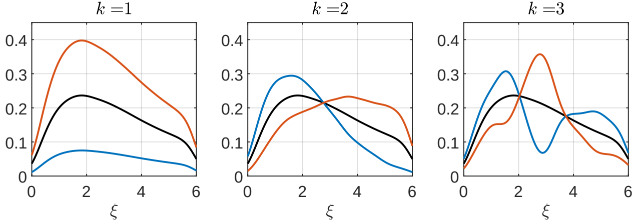

DGP's modes of variation: change to the mean distribution implied by a 2 std change in $\alpha_{k,t}$ (red: positive, blue: negative).

Simulated Data 3: Krusell and Smith (1998) DGP

- Simulated data borrowed from Chang M. et al. (2022);
- $T = 160$ artificial observations from the SVAR(1) resulting from the log-linearized solution of the Krusell and Smith (1998) model. Observe:
  - Productivity level, the capital stock, the employment level ($n_v = 3$);
  - Centered moments of the distribution of assets among the employed;
- A sample of $N = 9230$ is draws from the asset distribution;
- The matrix A_0 implied by the model is lower triangular, the first structural shock is a productivity shock.

Alternative Transformations of $p_t(\cdot)$

- Compare approximation provided by FPC when performed on different transformations of $p_t(\cdot)$;
- Cross-validation:
  1. Extract FPC from 80% of the (time) sample (randomly selected);
  2. Estimate the α_t for the remaining 20% of the sample through OLS;
  3. For this 20%, compute the Mean Integrated Squared Error for every K:

$$MISE = \frac{1}{T}\sum_{t=1}^{T}\int_{\Xi}\left(\hat{f}_t(\xi) - f_t(\xi)\right)^2 d\xi$$

  where $\hat{f}_t(\xi) = \zeta(\xi)' \hat{\alpha}_t$, with $\zeta(\xi)$ and $\hat{\alpha}_t$ being the FPC and scores estimated in point 1 and 2 above.

- The experiment is repeated 100 times for the first 2 DGPs.

Alternative Transformations of $p_t(\cdot)$

MISE

		K				
		1	2	3	4	5
DGP1	$p_t(\cdot)$	1	0.465	0.249	0.127	0.069
	$\log p_t(\cdot)$	1.879	1.457	0.996	0.730	0.594
	LQD	1.085	0.644	0.530	0.370	0.307
DGP2	$p_t(\cdot)$	1	0.102	0.053	0.032	0.022
	$\log p_t(\cdot)$	5.150	1.982	3.143	1.671	1.128
	LQD	2.334	1.167	0.678	0.421	0.337
DGP3	$p_t(\cdot)$	1	0.598	0.486	0.395	0.324
	$\log p_t(\cdot)$	1.908	1.857	1.467	1.339	1.260
	LQD	1.449	1.199	1.174	1.066	1.020

Ratios relative to the MISE attained by the first approach for $K = 1$.

Alternative Transformations of $p_t(\cdot)$: Comments

- FPCA on $p_t(\cdot)$ produces the best approximations in our DGPs;
- The average $\frac{1}{T}\sum_{t=1}^{T} p_t(\xi)$ has unit integral, while FPCs on $p_t(\cdot) - \frac{1}{T}\sum_{t=1}^{T} p_t(\xi)$ have zero integral by construction (therefore have negative regions). This implies that:
  - F-IRFs always integrate to 1;
  - If a shock moves the distribution away from the mean, the resulting distribution has negative regions;
- Common solution is to perform FPCA on $\log(p_t(\cdot))$;
- FPCA on the LQD allows approximations significantly more accurate than those based on $\log(p_t(\cdot))$;
- In the analysis, we use FPC extracted from the de-meaned LQD (results do not change if we follow the other approaches).

Interpretation of F-IRFs

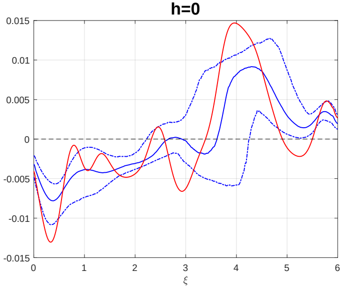

- The figure shows the difference between $p_{ss+h}(\cdot)\,|_{\varepsilon_j = std(\varepsilon_j)}$ and $p_{ss}(\cdot)$.
  - The horizontal axis shows the support Ξ;
  - The vertical axis mesures the difference between the two densities;
  - h is the horizon of the response.

F-SVAR DGP 1: F-IRFs

Single realization of the simulated experiment.
Red lines: true responses of $p_t(\cdot)$ to one standard deviation shocks to ε_1 (upper panels) and ε_2 (lower panels). Solid blue lines: posterior median responses, dashed blue lines: 90% credible bands. h denotes the horizon at which the response is measured.The number of FPC is selected as the smallest one for which 90% of variance is explained.

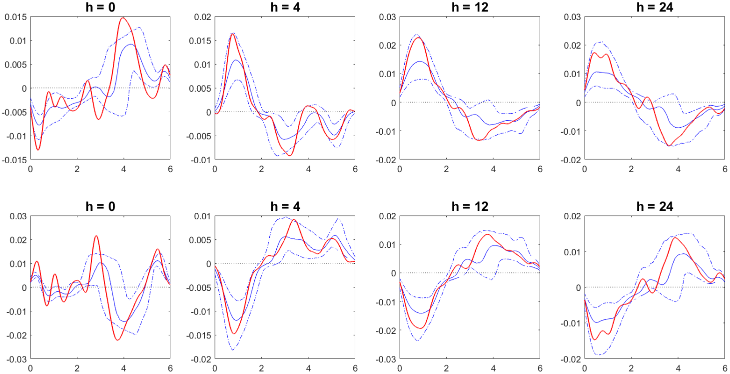

F-SVAR DGP 2: F-IRFs

Red lines: true responses of $p_t(\cdot)$ to one standard deviation shocks to ε_1 (upper panels) and ε_2 (lower panels). Solid blue lines: posterior median responses, dashed blue lines: 90% credible bands. h denotes the horizon at which the response is measured.The number of FPC is selected as the smallest one for which 90% of variance is explained.

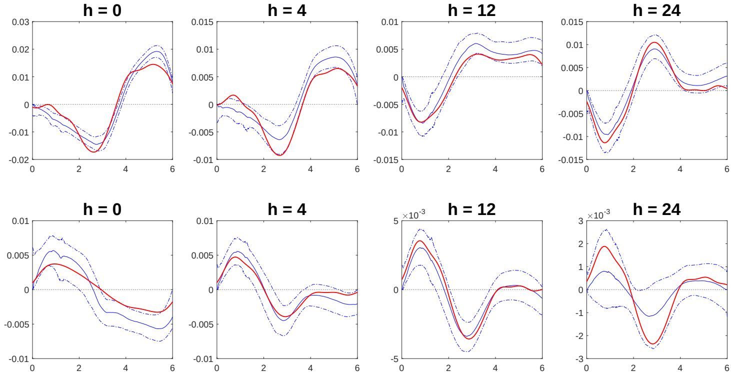

Krusell and Smith (1998) DGP: F-IRFs

Red lines: true responses of $p_t(\cdot)$ to one standard deviation technology shocks. Solid blue lines: posterior median responses, dashed blue lines: 90% credible bands. The number of FPC is selected as the smallest one for which 90% of variance is explained. (Timing convetion is different than the one in Chang et al.(2024): here shock happens at $t = 0$, there at $t = 2$)

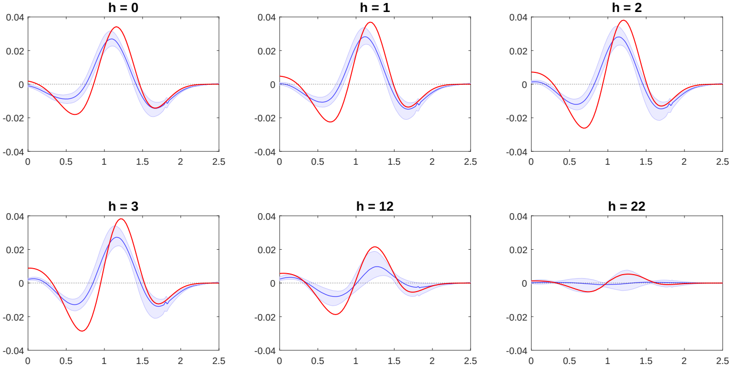

Monte Carlo: F-SVAR DGP 1

Average correlation between median and true F-IRFs across 200 MC replications.

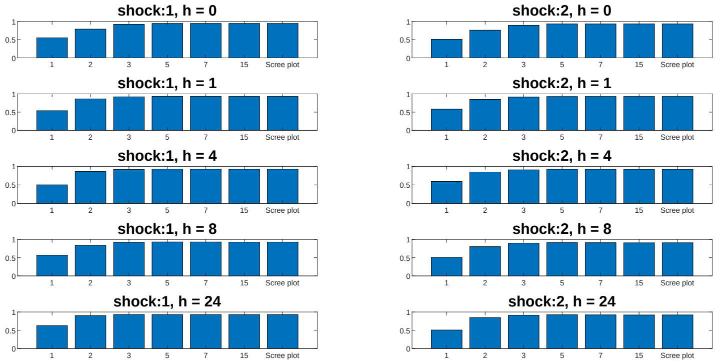

Horizontal axis reports number of FPC (K). Scree Plot: select K so that 90% of variance is explained

Monte Carlo: F-SVAR DGP 2

Average correlation between median and true F-IRFs across 200 MC replications.

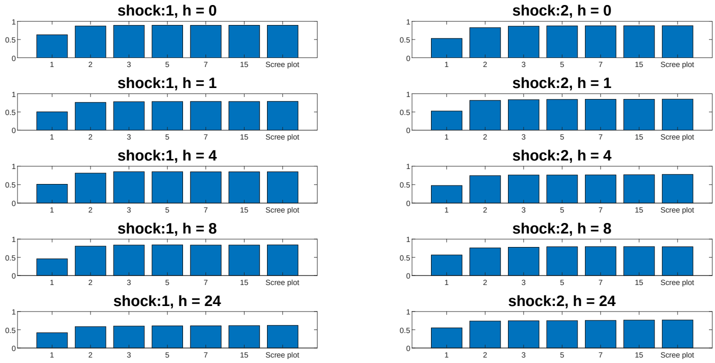

Horizontal axis reports number of FPC (K). Scree Plot: select K so that 90% of variance is explained

Uncertainty shocks: the model

- Augment the VAR model analyzed by Jurado et al. (JLN, 2015) by including the income distribution among employed people as $f_t(\cdot)$;
- Earnings-to-GDP data constructed by Chang M et al. (2022) based on the Current Population Survey (CPS);
- Support of the distribution is $\Xi = [0, 2.1]$ (2.1 is the smallest censoring point in the sample);
- Convert the monthly SVAR of JLN in a quarterly F-SVAR model and focus on the period 1989:Q1 - 2017:Q3;
- The $n_v = 11$ endogenous variables included in the model are: (i) real GDP, (ii) real PCE, (iii) GDP deflator, (iv) real wages, (v) real investments, (vi) labor productivity, (vii) unemployment rate, (viii) Federal Funds Rate, (ix) S&P500 index, (x) M2 growth rate, and (xi) JLN's macro-uncertainty measure;
- Assume $K = 7$ (different Ks do not affect results for $K > 2$);
- The macro-uncertainty shock is identified by ordering the uncertainty measure last among the aggregate variables in a Cholesky identification scheme.

Income Distribution: Scree Plot

Share of variance explained by FPC.

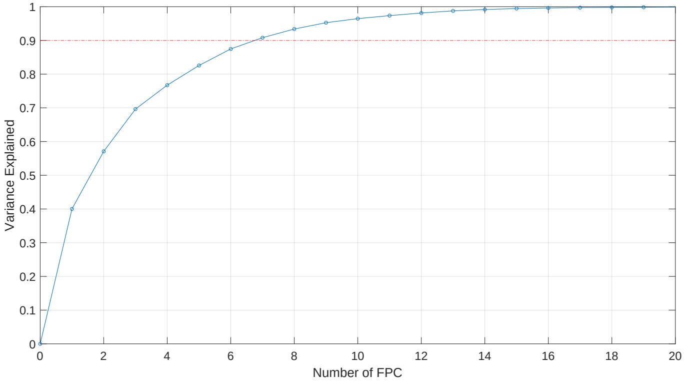

Uncertainty shocks: IRFs

IRFs to an uncertainty shock implied by: a SVAR (red), F-SVAR (blue), 68% credible bands (dashed lines and shaded areas).

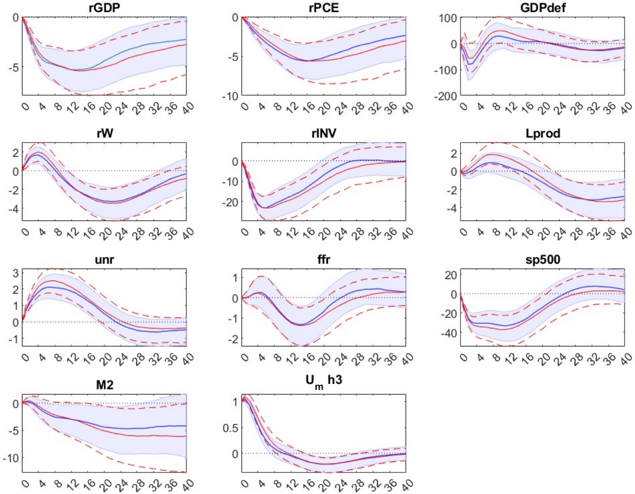

Uncertainty shocks: F-IRFs

Response of income distribution to an uncertainty shock:

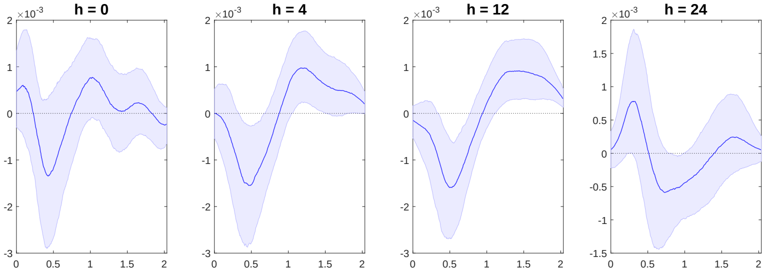

- The horizontal axis measures the earnings relative to the per-capita level of GDP;
- *h* denotes the horizon in quarters.

Uncertainty shocks: comments

- Aggregate effects:
  - IRFs predicted by the F-SVAR are similar to those generated by the standard SVAR, but:
    - Response of inflation is negative;
    - Labor productivity is not affected in the short run.
- Distributional effects:
  - Propagation two phases:
    - In the short run (up to 12 moths): while unemployment increases, the share of workers with low relative income decreases, and the mass of people employed receiving income above the average increases;
    - In the longer run: while unemployment is reabsorbed, the share of occupied with low relative income increases to the detriment of the middle-income class (probably due to the decrease of labor productivity triggered by the decrease in investments experienced at short horizons).

Uncertainty shocks: Quantiles IRF

The F-IRFs of income distribution can be mapped to the IRF of quantiles of interest:

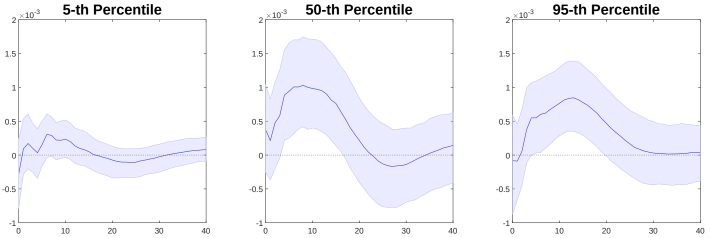

- The horizontal axis indicates the horizon in quarters, the vertical axis measures the change in the quantile.
- While the bottom quantile is affected only mildly, the median and the top quantiles shift to the right significantly.

Uncertainty shocks: Earning Classes IRF

The F-IRFs of income distribution can be mapped to the response of the share of employed people belonging to specific earnings classes:

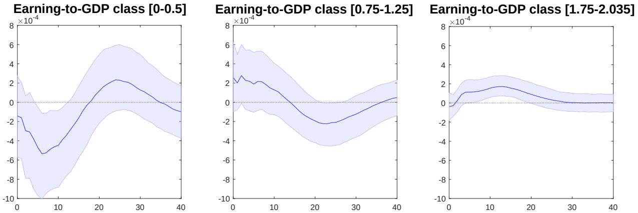

- The share of employed people belonging to the low-income class decreases significantly in a first phase, while the relative weight of the middle and upper class increases;
- In a second phase, the share of low-income employed increases, drawing mainly from the middle class.

Uncertainty shocks: Gini IRF

The F-IRFs of income distribution can be mapped to the IRF of the Gini coefficient:

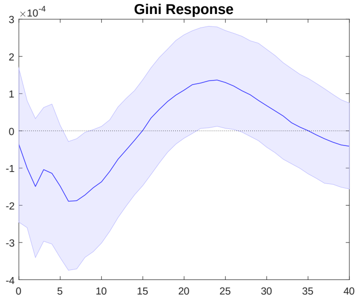

- Earnings inequality decreases in the short run, but it increases at longer horizons.

Uncertainty shocks: Interpretation

- The decline of the share of people earning low income is due to a stronger rise in unemployment among low income classes;
- We add to the monthly JLN VAR unemployment rates by educational attainment:

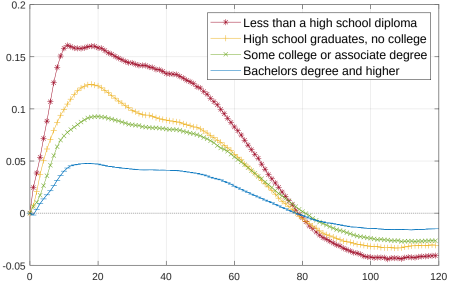

Further developments: Functional LP

- F-IRFs can be also estimated by Local Projections;
  1. Estimate responses of α_t:
     $IR_\alpha(t, h, d_i) = E[\alpha_{t+h} \mid \varepsilon_t = d_i, \Im_t] - E[\alpha_{t+h} \mid \varepsilon_t = 0, \Im_t]$;
  2. Compute the Functional IRFs through the mapping:
     $IR_f(\xi, t, h, d_i) = \zeta'(\xi) \times IR_\alpha(t, h, d_i)$;

  Suppose y_{1t} is predetermined w.r.t. $[y_{2t}, \ldots, y_{n_v t}, \alpha_t]'$.
  The joint response of α to an impulse in y_1 can be estimated through the multivariate regression:

$$\alpha_{t+h} = a^h + \beta_1^h y_{1,t} + \sum_{l=1}^{p} B_{l+1}^h \left[\begin{array}{cc} y'_{t-l}, & \alpha'_{t-l} \end{array} \right]' + e_{h,t}$$

  where $IR_\alpha(t, h, d_i = [1, 0, \ldots, 0]') = \beta_1^h$.
- Can be estimated by OLS with (system-wide) HAR standard errors.

F-LP DGP 1: F-IRFs

Red lines: true responses of $p_t(\cdot)$ to one standard deviation shocks to ε_1 (upper panels) and ε_2 (lower panels). Solid blue lines: posterior median responses, dashed blue lines: 90% credible bands. h denotes the horizon at which the response is measured.The number of FPC is selected as the smallest one for which 90% of variance is explained.

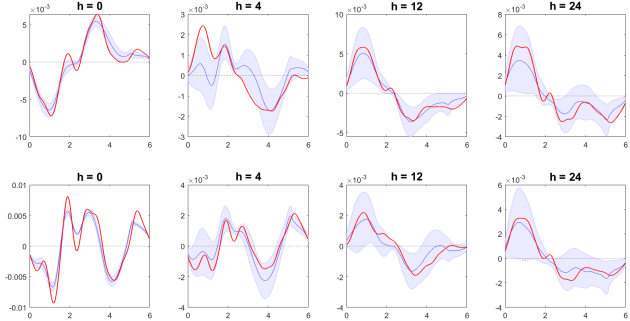

DGP 1: F-LP vs F-SVAR

Blue Lines: F-LP. Red lines: F-SVAR.

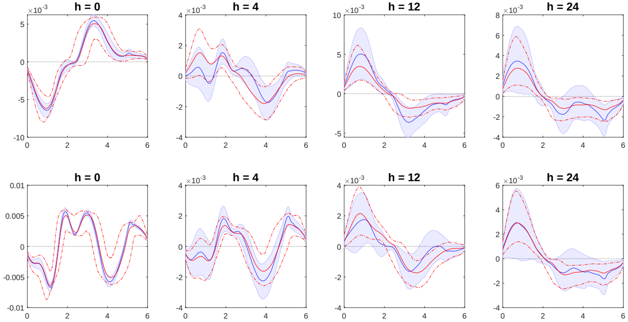

F-LP DGP 2: F-IRFs

Red lines: true responses of $p_t(\cdot)$ to one standard deviation shocks to ε_1 (upper panels) and ε_2 (lower panels). Solid blue lines: posterior median responses, dashed blue lines: 90% credible bands. h denotes the horizon at which the response is measured.The number of FPC is selected as the smallest one for which 90% of variance is explained.

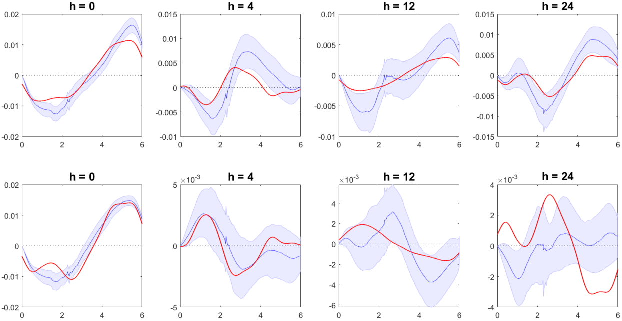

DGP 2: F-LP vs F-SVAR

Blue Lines: F-LP. Red lines: F-SVAR.

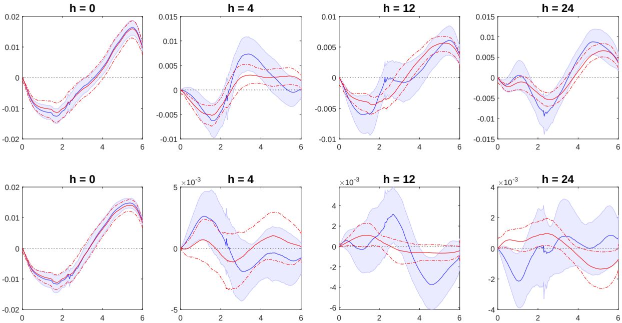

Krusell and Smith (1998) DGP: F-IRFs

F-IRFs of the asset distribution to a productivity shock: implied by the DGP (red), estimated (solid blue), and 90% confidence intervals (dotted blue).

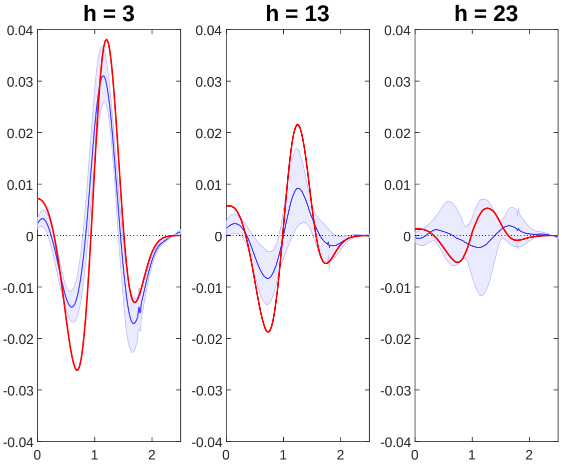

Uncertainty Shocks: F-IRFs

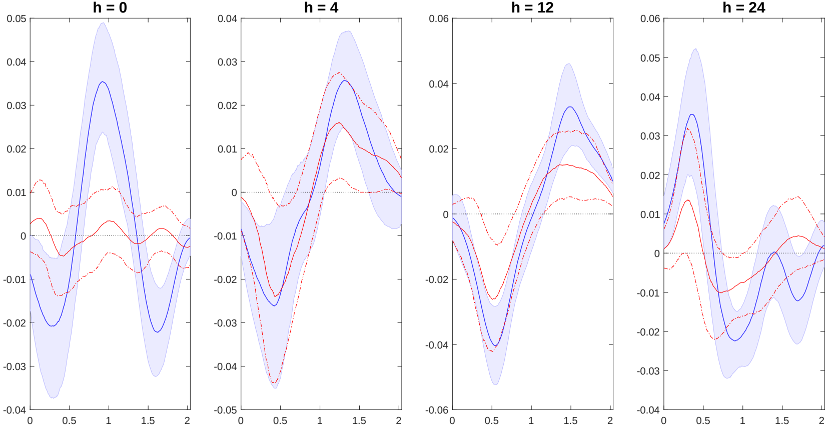

Conclusion

- Proposed a F-VAR to jointly study aggregate variables and distributions, where the latter are approximated by FPCA.
- Compared FPCA based on different transformations of the distribution of interest;
- Assessed the performance of the Bayesian inference method in simulation experiments;
- Studied the distributional implications of uncertainty shocks. Propagation of uncertainty shocks has two phases:
  - Short run: unemployment increases and share of employed with low relative income decreases;
  - Longer horizon: unemployment is reabsorbed, but mass of low-income workers grows, increasing inequality.
- All F-IRFs can be estimated by Functional Local Projections;
- Related ongoing research: (i) Bi-variate distributions (e.g. firms labor and capital), (ii) Nowcasting income/consumption distributions.

Thank You!

Ahn, S., Kaplan, G., Moll, B., Winberry, T., and Wolf, C., 2018. "When Inequality Matters for Macro and Macro Matters for Inequality," in *NBER Macroeconomics Annual* 2017, pp. 1-75;

Anderson, E., Inoue, A., and Rossi, B., 2016. "Heterogeneous Consumers and Fiscal Policy Shocks," *Journal of Money, Credit and Banking* 48(8), 1877-1888;

Athreya, K. B., Owens, A., Romero, J. S., and Schwartzman, F., 2017. "Does Redistribution Increase Output?," *Richmond Fed Economic Brief*, issue January;

Auclert, A., and Rognlie, M., 2020. "Inequality and Aggregate Demand," Manuscript, Stanford University;

Bloom, N., 2009. "The impact of uncertainty shocks." *Econometrica*, 77(3), 623-685;

Bjornland, H. C., Chang, Y., and Cross, J. L., 2023. "Oil and the Stock Market Revisited: A Mixed Functional VAR Approach," *CAMA Working Papers* 2023-18;

- Carriero, A., Clark, T. E., & Marcellino, M., 2015. Bayesian VARs: specification choices and forecast accuracy. *Journal of Applied Econometrics*, 30(1), 46-73;
- Carriero, A., Clark, T.E., Marcellino, M., 2021. Using time-varying volatility for identification in Vector Autoregressions: An application to endogenous uncertainty. *Journal of Econometrics*, Elsevier 225 (1), 47–73;
- Carriero, A., Marcellino, M., and Tornese, T. 2023. Macro uncertainty in the long run. Economics Letters, 225, 111067;
- Castelnuovo, E., 2019. "Domestic and Global Uncertainty: A Survey and Some New Results." *CESifo Working Paper Series* 7900, CESifo;
- Chang, M., Chen, X., & Schorfheide, F., 2024. "Heterogeneity and Aggregate Fluctuations." *Journal of Political Economy*, Forthcoming;
- Chang, Y., Gomez-Rodrguez, F., and Hong, M. G. H., 2022. "The Eeffcts of Economic Shocks on Heterogeneous Inflation Expectations." International Monetary Fund;
- Chang, Y., Kim, C. S., & Park, J. Y., 2016. "Nonstationarity in time series of state densities." *Journal of Econometrics*, 192(1), 152-167;
- Diebold, F. X., and Li, C., 2006 "Forecasting the term structure of government bond yields." *Journal of Econometrics,* 130(2): 337-364;

- De Giorgi, G., ans Gambetti, L., 2017. "Business Cycle Fluctuations and the Distribution of Consumption," *Review of Economic Dynamics*, 23, 19-41;
- Doan, T., Litterman, R., & Sims, C., 1984. "Forecasting and conditional projection using realistic prior distributions." *Econometric reviews*, 3(1), 1-100;
- Heathcote, J., Storesletten, K., and Violante, G. L., 2010. "The Macroeconomic Implications of Rising Wage Inequality in the United States," *Journal of Political Economy*, 118(4), 681-722;
- Fernández-Villaverde, Jesús and Pablo A. Guerrón-Quintana. "Uncertainty shocks and business cycle research." *Review of Economic Dynamics* 37 (2020): S118 - S146;
- Ferraty, F., and Vieu, P. (2006), *Nonparametric Functional Data Analysis: Theory and Practice*, NewYork: Springer. [733];
- Hu, B., & Park, J. Y., 2017. "Econometric Analysis of Functional Dynamics in the Presence of Persistence." Manuscript, Department of Economics, Indiana University;
- Inoue, A., and Rossi, B., 2021. "The Effects of Conventional and Unconventional Monetary Policy: A New Approach." *Quantitative Economics*, 12(4), 1085-1138;
- Jurado, K., Ludvigson, S. C., & Ng, S., 2015. "Measuring uncertainty." *American Economic Review*, 105(3), 1177-1216;

- Kaplan, G., and L. Violante, G. L., 2018. "Microeconomic Heterogeneity and Macroeconomic Shocks." *Journal of Economic Perspective*, 32, 167-194;
- Kowal, D. R., Matteson, D. S., and Ruppert, D. 2017. "A Bayesian Multivariate Functional Dynamic Linear Model." *Journal of the American Statistical Association*, 112, 733–744;
- Krusell, P., and Smith, A. A., 1998. "Income and Wealth Heterogeneity in the Macroeconomy." *Journal of Political Economy*, 106(5), 867-896;
- Litterman, R. B. & Scheinkman J. 1991. "Common Factors Affecting Bond Returns." *The Journal of Fixed Income*, 1 (1);
- Meeks, R., ans Monti, F., 2019. "Heterogeneous beliefs and the Phillips curve." *Bank of England working papers* 807, Bank of England;
- Petersen, A., and H.-G. Muller (2016): "Functional data analysis for density functions by transformation to a Hilbert space," *Annals of Statistics*, 44, 183–218.
- Tsay, R. S., 2016. "Some Methods for Analyzing Big Dependent Data," *Journal of Business & Economic Statistics*, 34(4), 673-688;
- Venables, W. N., Ripley, B. D., 1999. *Univariate statistics*. Modern Applied Statistics with S-PLUS, 113-148.